Formation and quenching kinetics of electron beam excited Xe_2Br^*

W. L. Wilson, Jr., R. A. Williams, R. Sauerbrey,[a] F. K. Tittel, and G. Marowsky[b]

Department of Electrical Engineering and Rice Quantum Institute, Rice University, Houston, Texas 77251
(Received 8 February 1982; accepted 4 May 1982)

Formation and quenching processes, as well as the optical emission characteristics of Xe_2Br^*, centered at 440 ± 30 nm were investigated for electron beam pumped mixtures of argon, xenon, and several different bromine donors. Three-body collisional quenching of XeBr* was identified as the primary formation mechanism for the triatomic species. Quenching rates for Xe_2Br^* and XeBr* were measured and the Xe_2Br^* radiative lifetime was determined to be 245 ± 30 ns.

INTRODUCTION

In recent years there has been considerable interest in the triatomic rare gas–halogen excimers.[1–5] These excimers exhibit radiative transitions in the wavelength region from 260 to 650 nm. Because the triatomic rare gas–halogens have a steeply repulsive potential energy curve in the ground state, the fluorescence is inherently broadband, as compared to the narrow spectral linewidth of the diatomic excimer.

The existence of the triatomic excimers was first identified from companion fluorescence observed on the long wavelength side of the emission from their diatomic counterparts.[1,3] These trimers were first viewed as a loss mechanism for the diatomic rare gas–halide lasers.[6–9] It was proposed by Huestis *et al.*[10] that these triatomic molecules could be employed as tunable laser media. Subsequently, electron beam excited Xe_2Cl^* was shown to have optical gain within its fluorescence band.[11] Two triatomic lasers Xe_2Cl^* centered at 520 nm and Kr_2F^* centered at 435 nm were demonstrated by Tittel *et al.*[5,12,13]

In this paper, we describe the excited state kinetics of the triatomic rare gas halide Xe_2Br^*. This excimer was investigated in order to establish the feasibility of a Xe_2Br^* laser. Furthermore, the formation of Xe_2Br^* represents an important loss mechanism for the XeBr* laser.

Narrow band emission from the diatomic species, XeBr* was first reported by Velazco and Setser[14] and Brau and Ewing.[15] XeBr* was the first diatomic excimer for which laser action was demonstrated.[16] The fluorescence emission spectrum of the triatomic species, Xe_2Br^* was recently reported by Konovalov *et al.*[17]

In our experiments, the trimer Xe_2Br^* was formed by electron beam excitation of high pressure mixtures of argon, xenon, and a bromine donor. Figure 1 illustrates typical fluorescence emission from an electron beam pumped mixture of Xe, Ar, and Br_2. The XeBr $(B \rightarrow X)$ emission at 282 nm, the Br_2^* emission at 291 nm, and the very broadband Xe_2Br^* emission centered at 440 nm are depicted in the figure. The fluorescence intensity and decay rate of the Xe_2Br^* emission were studied as a function of gas mixture in order to determine the quenching behavior of the constituents, and the radiative lifetime of the trimer. From this data, a kinetic model for the formation and removal of the triatomic excimer was developed.

EXPERIMENTAL PROCEDURE

Mixtures of high purity argon (99.999%) (0.5 to 6 atm), xenon (50 to 900 Torr), and various bromine donor gases (0.1 to 5 Torr) in a stainless steel reaction cell were transversly pumped by an electron beam. The 10 ns long beam of 1 MeV electrons was generated by a Physics International Pulserad 110 accelerator, and typically had a maximum current density of 200 A/cm^2 at the optical axis of the cell. Details of the apparatus and experimental techniques employed have been described elsewhere.[5,18]

The optical emission from the cell was monitored with two fast vacuum photodiodes (ITT F4000S). Interference and color glass filters were used to define the spectral region of interest (280 and 450 nm) for each diode. The photodiode signals were recorded with a Tektronix 7912 transient digitizer, with a time resolution of about 3 ns. A 0.25 m Jarrell-Ash spectrometer, in connection with

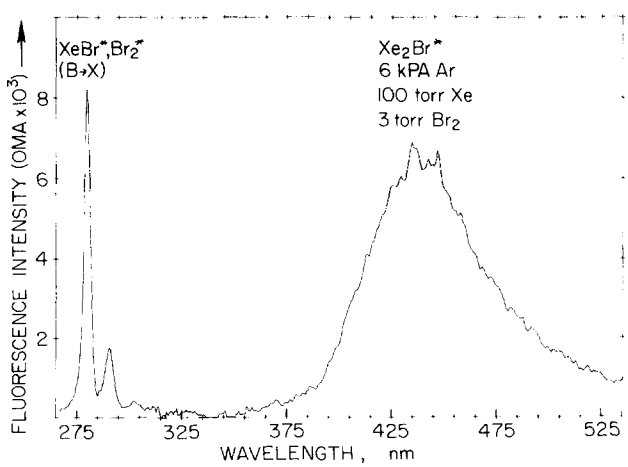

FIG. 1. Fluorescence spectrum of electron beam excited mixture of Ar/Xe/Br_2. The broadband Xe_2Br^* emission centered 440 nm is seen together with XeBr* emission at 282 nm, and Br_2^* at 291 nm.

[a] Permanent address: Physikalisches Insitut der Universitat Wurzburg, Wurzburg, West Germany.

[b] Max-Planck Institut fur biophysikalische Chemie, Abteilung Laserphysik, West Germany.

 0021-9606/82/161830-07$02.10

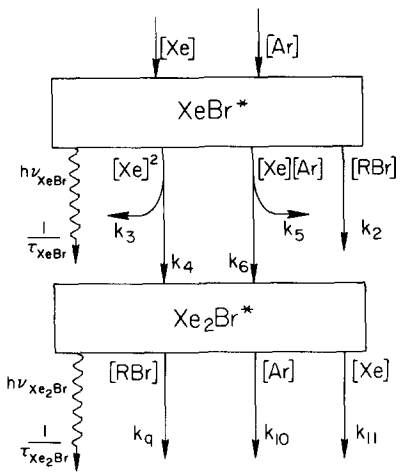

FIG. 2. Kinetic model for the $XeBr^*$–Xe_2Br^* system.

an OMA-1 optical multichannel analyzer, was used to observe temporally integrated emission spectra. Both the transient digitizer and the OMA-1 were interfaced to a DEC 11/23 minicomputer. Computer software allowed integration of the OMA data over various spectral regions, and temporal integration of the photodiode signals. Least-squares fitting to the decay of the photodiode signal permitted accurate determination of the Xe_2Br^* decay time as a function of the partial pressures of argon, xenon and the bromine donor.

KINETIC MODEL

From fluorescence measurements it is possible to characterize the formation kinetics, quenching processes, and donor efficiency for an excimer system. Based on the data to be presented below, and in analogy with other triatomic excimer systems which have been studied,[19–25] the most likely formation route for Xe_2Br is via the diatomic excimer $XeBr^*$, as illustrated in Fig. 2.

In the case of e-beam excitation, the primary formation mechanism for $XeBr^*$ is via a harpooning reaction between the xenon metastable Xe^*, and the bromine donor molecule RBr[26] and ionic reactions of Xe_2^+ with Br^-. Xe^* is removed by a termolecular reaction with Ar and Xe to form Xe_2^*. The primary quenching pathways for Xe_2^* are radiation and possibly, reaction with a donor to form Xe_2Br^*. This formation channel for the trimer molecule has been observed in the case of Ar_2F^* by Chen *et al.*,[19] and by Bowering *et al.*[22]

The most important reactions involving $XeBr^*$, leading to the formation of Xe_2Br^* are listed in Table I. The removal of $XeBr^*$ can occur via radiative decay [Reaction (1)], as well as through interaction with the other constituents of the gas mixture [Reactions (2)–(7)]. However, only two of these reactions result in the production of Xe_2Br^* [Reactions (4) and (6)]. The rate constants for Reactions (4) and (6) are both of the same order of magnitude (see below), but because in most of the experiments the argon pressure is much higher than the xenon reaction, Reaction (6) dominates.

Assuming linear quenching for Xe_2Br^*, and neglecting a possible production channel for Xe_2Br^* via Xe_2^*, the following rate equation describing the time dependence of the Xe_2Br^* population is obtained:

$$\frac{d}{dt}[Xe_2Br^*] = (k_6[Ar] + k_4[Xe])[Xe][XeBr^*] - \frac{1}{\tau_{eff}}[Xe_2Br^*]. \tag{1}$$

In this equation, the quantities in brackets (e.g., [Xe]) represents the density of that species in the gas mixture. The rate constants for the formation reaction are given by k_6 and k_4 (see Table I) and τ_{eff} is the effective decay time of Xe_2Br^*, which will be discussed below. For sufficiently low xenon pressures, the xenon–xenon formation reaction [given as Reaction (4) in Table I] can be neglected, and Eq. (1) can be integrated to yield

$$[Xe_2Br^*(t)] = k_6[Ar][Xe]\int_0^t [XeBr^*(t')]\,dt' - \frac{1}{\tau_{eff}}\int_0^t [XeBr^*(t')]\,dt' . \tag{2}$$

The observed time integrated fluorescence intensities in the UV and visible I_{UV} and I_{vis} are given by

TABLE I. Formation and quenching reactions for $XeBr^*$ and Xe_2Br^*.

	Reaction	Rate constant	Reference
1.	$XeBr^* \rightarrow Xe + Br + h\nu_{XeBr}$	$\tau_{XeBr} = 17.5$ ns	27
2.	$XeBr^* + RBr \rightarrow$ products	$k_2 = 8\times10^{-10}$ cm^3 s^{-1} [a]	27
3.	$XeBr^* + 2Xe \rightarrow$ products	$k_3 + k_4 = (2.7 \pm 0.9)\times10^{-31}$ cm^6 s^{-1}	This work
4.	$XeBr^* + 2Xe \rightarrow Xe_2Br^* + Xe$	$k_4 \approx 2.7\times10^{-31}$ cm^6 s^{-1}	This work
5.	$XeBr^* + Ar + Xe \rightarrow$ products	$k_5 + k_6 = (3.0 \pm 0.8)\times10^{-31}$ cm^6 s^{-1}	This work
6.	$XeBr^* + Ar + Xe \rightarrow Xe_2Br^* + Ar$	$k_6 = (3.2 \pm 0.4)\times10^{-31}$ cm^6 s^{-1}	This work
7.	$XeBr^* + Ar + Xe \rightarrow$ other products	$k_5 \leq 1\times10^{-31}$ cm^6 s^{-1}	This work
8.	$Xe_2Br^* \rightarrow 2Xe + Br + h\nu_{Xe_2Br}$	$\tau_{Xe_2Br} = 245 \pm 30$ ns	This work
9.	$Xe_2Br^* + RBr \rightarrow$ products	see Table II for k_q	This work
10.	$Xe_2Br^* + Ar \rightarrow$ products	$k_{10} \leq 2\times10^{-14}$ cm^3 s^{-1}	This work
11.	$Xe_2Br^* + Xe \rightarrow$ products	$k_{11} = (2.8 \pm 0.9)\times10^{-13}$ cm^3 s^{-1}	This work

[a] For donor Br_2.

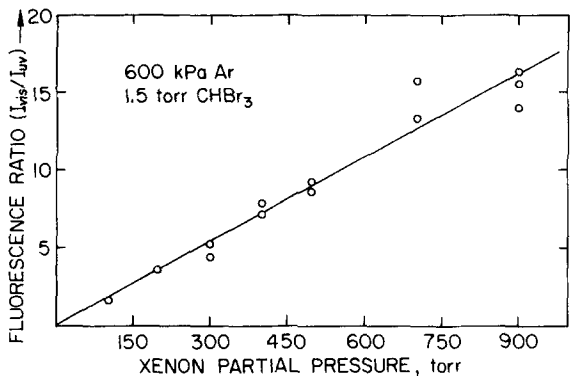

FIG. 3. Ratio of the time and wavelength integrated fluorescence intensity of the visible emission at 440 nm to the UV emission at 282 nm as a function of xenon pressure for argon, xenon, and $CHBr_3$ mixtures.

$$I_{UV} = C_1 \int_0^\infty [XeBr^*(t')]\,dt' \ , \tag{3}$$

$$I_{vis} = C_2 \int_0^\infty [Xe_2Br^*(t')]\,dt' . \tag{4}$$

The constants C_1 and C_2 contain the radiative lifetimes of $XeBr^*$ and Xe_2Br^*, as well as the spectral sensitivity of the detection system. The Xe_2Br^* population will decay to zero after sufficient time. Thus, if we set $t=\infty$ in Eq. (2), the left-hand side is zero, and then substituting Eqs. (3) and (4) we obtain

$$\frac{I_{vis}}{I_{UV}} = \frac{C_2}{C_1} k_6 \tau_{eff} [Xe][Ar] \ . \tag{5}$$

These intensities are directly measured with the optical multichannel analyzer, when the spectra are integrated over the appropriate UV and visible wavelengths. Figure 3 shows the intensity ratio as a function of xenon pressure. The linear dependence of the intensity ratio on the xenon pressure supports the assumption that Reaction (6) is the primary production channel for Xe_2Br^*.

Formation of Xe_2Br^*

In order to study the formation mechanism of Xe_2Br^* in detail, the time dependence of the Xe_2Br^* and $XeBr^*$ fluorescence was investigated. The time dependence of the fluorescence signals, as measured by the photodiodes, is given by

$$V_{XeBr}(t) = \alpha_1 \frac{[XeBr^*(t)]}{\tau_{XeBr}} \ , \tag{6}$$

$$V_{Xe_2Br^*}(t) = \alpha_2 \frac{[Xe_2Br^*(t)]}{\tau_{Xe_2Br}} \ . \tag{7}$$

The constants α_1 and α_2 contain the transmission characteristics of the filters used to separate the UV and the visible fluorescence, which were very carefully determined, and the sensitivity of the photodiode for the different wavelengths. Substituting Eqs. (6) and (7) into Eq. (1), and neglecting the $k_4[Xe][Xe]$ term as compared to the $k_6[Xe][Ar]$ term, we find

$$\frac{d}{dt} V_{Xe_2Br^*} = k_6[Ar][Xe] \frac{\alpha_2}{\alpha_1} \frac{\tau_{XeBr}}{\tau_{Xe_2Br}} V_{XeBr} - \frac{1}{\tau_{eff}} V_{Xe_2Br} \ . \tag{8}$$

The constants k_6 and τ_{eff} can be determined by fitting the Xe_2Br^* fluorescence signal obtained by integrating Eq. (8) to the observed Xe_2Br^* fluorescence. The measured $XeBr^*$ emission is used as input data for the integration. To insure good time synchronization between the input $XeBr^*$ pulse and the Xe_2Br^* pulse to be fit, the same photodiode was used to obtain both signals, the interference filters were simply interchanged, leaving everything else in the experiment constant. Figure 4 shows a typical $XeBr^*$ fluorescence pulse at 282 nm and the observed Xe_2Br^* emission at 450 nm. The dashed curve in Fig. 4 is the result of a computer integration of Eq. (8), with $k_6 = 3.1\times10^{-31}$ cm^6 s^{-1}. Fits for a number of different gas mixtures, resulted in a formation constant k_6 of $(3.2\pm0.4)\times10^{-31}$ cm^6 s^{-1}. This value also agrees to within 20% to the value one gets by substituting for C_2/C_1 and τ_{eff} in Eq. (5).

Further insight into the processes leading to the formation of Xe_2Br^* can be obtained by looking at the removal of $XeBr^*$. Neglecting the inefficient two-body quenching by the rare gases, the pertinent rate equation for the dimer can be written as

$$\frac{d[XeBr^*]}{dt} = P - \{k_2[RBr] + (k_3+k_4)[Xe][Xe] + (k_5+k_6)[Ar][Xe] + (1/\tau)\}[XeBr^*] \ . \tag{9}$$

In this equation, P is the net production rate of $XeBr^*$ and τ is the radiative lifetime of $XeBr^*$. In our pressure regime, the production of $XeBr^*$ is much faster than the production of either Ar_2^* or Xe_2^*, and P can be written as

$$P = f_1[Ar] + f_2[Xe] \ . \tag{10}$$

The constants f_1 and f_2 represent the formation constants for $XeBr^*$ as a result of the argon and xenon concentration in the cell. This assumption will be discussed in detail below. With the argon concentration set to zero, and taking the time dependent $XeBr^*$ fluorescence at its peak (when the derivative is zero), one can put Eq. (9) in the following form:

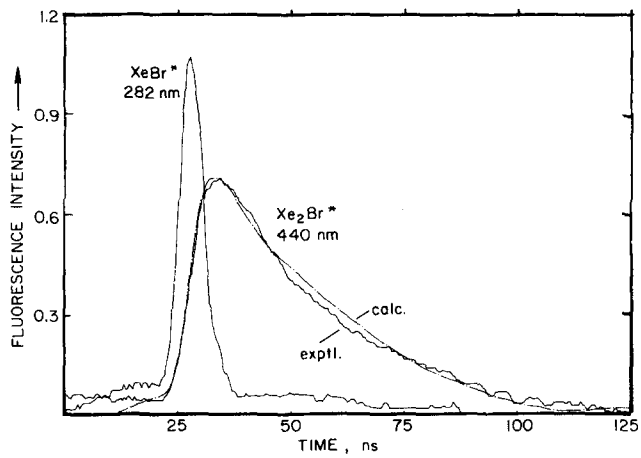

FIG. 4. Temporal behavior of the ultraviolet $XeBr^*$ emissions at 282 nm and the visible Xe_2Br^* emission at 440 nm for a mixture of 2 Torr $CHBr_3$, 100 Torr Xe, and 600 kPa Ar. The dotted curve results from an integration of the $XeBr^*$ pulse, using appropriate formation and quenching rates.

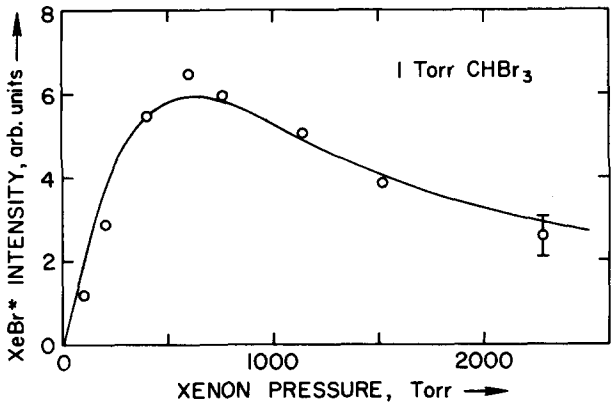

FIG. 5. XeBr* fluorescence peak intensity as a function of xenon pressure for a mixture of 1 Torr $CHBr_3$ and xenon. The solid line is the result of a fit of Eq. (11) to the data.

$$[XeBr^*] = \frac{f_2[Xe]}{k_2[RBr] + (k_3 + k_4)[Xe][Xe] + (1/\tau)} . \quad (11)$$

Using $(1/\tau) + k_2[RBr] = 1.0 \times 10^8\ s^{-1}$[27] a fit was made of the curve obtained by observing the peak in the XeBr* emission as a function of xenon pressure with no argon present (Fig. 5). The fit yields the parameters f_2 and $(k_3 + k_4)$.

Returning to Eq. (9) and again letting the derivative equal zero, the following expression for the peak of the XeBr* emission is obtained when both argon and xenon are present:

$$[XeBr^*] = \frac{f_1[Ar] + f_2[Xe]}{k_2[RBr] + (k_3 + k_4)[Xe][Xe] + (k_5 + k_6)[Xe][Ar] + (1/\tau)} . \quad (12)$$

With this equation, a fit is made to a plot of XeBr* emission as a function of argon pressure, with a fixed xenon pressure. Since τ, k_2, $(k_3 + k_4)$, and f_2 are known the two parameters f_1 and $(k_5 + k_6)$ can now be determined. Such a fit is shown in Fig. 6 for two different xenon concentrations. The same rate constants were used to fit both curves. The constants determined from this analysis are $(k_5 + k_6) = (3.0 \pm 0.8) \times 10^{-31}\ cm^6\ s^{-1}$ and $(k_3 + k_4) = (2.7 \pm 0.9) \times 10^{-31}\ cm^6\ s^{-1}$.

Quenching and fluorescence characteristics of Xe_2Br^*

Quenching of Xe_2Br^* results from radiation and collisional interactions with the other species in the cell. The dominant quenching reactions are shown in Table I as Reactions (8)–(11). The observed decay of the Xe_2Br^* fluorescence tail was always of an exponential form, so the quenching constants can be found by monitoring the effective decay rate, τ_{eff} of the Xe_2Br^* fluorescence. This effective lifetime is given by

$$\tau_{eff}^{-1} = \tau_{Xe_2Br}^{-1} + k_q[RBr] + k_{10}[Ar] + k_{11}[Xe] . \quad (13)$$

The three quenching constants k_q, k_{10}, and k_{11}, are found by taking the slope of the Xe_2Br^* fluorescence decay rate plotted against the partial pressure of each of the quenchers. For example, the data for various mixtures of $Ar/Xe/CHBr_3$ are shown in Figs. 7(a)–7(c). For the quenching of Xe_2Br^* by Xe [Fig. 7(b)] a rate constant, $k_{11} = (2.8 \pm 0.9) \times 10^{-13}\ cm^3\ s^{-1}$ was determined. The quenching of Xe_2Br^* by Ar was significantly smaller and only an upper limit of $k_{10} < 2 \times 10^{-14}\ cm^3\ s^{-1}$ could be estimated from Fig. 4(c).

Quenching by the bromine donor molecule is dependent on the particular donor species used. Those donors which we investigated were CBr_4, $CHBr_3$, HBr, Br_2, CH_3Br, C_2H_5Br, and $C_6F_4Br_2$. Quenching values for many of the donors studied are given in Table II. Using the quenching constants determined above, a radiative lifetime τ_{Xe_2Br} of 245 ± 30 ns is determined from Eq. (13).

The Xe_2Br^* peak fluorescence intensity was investigated as a function of the various components in the gas mixture. The fluorescence increased with increasing xenon pressure up to about 200 Torr, after which the fluorescence intensity saturated. No further increase was observed up to 500 Torr xenon. The peak fluorescence intensity increased linearly with argon pressure up to 5 atm after which it saturated.

The fluorescence from various donor species was studied to determine which would yield optimum Xe_2Br^* emission. Carbon tetrabromide (CBr_4) had the highest fluorescence yield of the donors studied, but is a solid at room temperature, with a vapor pressure of only 0.5 Torr. In order to achieve a sufficient vapor pressure to conduct experiments, the entire cell must be heated to about 50 °C. The next best donor in terms of fluorescence yield, was bromoform ($CHBr_3$), which gave about 80% of the maximum yield of CBr_4. Since this donor has a vapor pressure of over 20 Torr at room temperature, it was experimentally more convenient to use than $CHBr_3$. Elemental bromine (Br_2) demonstrated only about 30% of the output of carbon tetra-

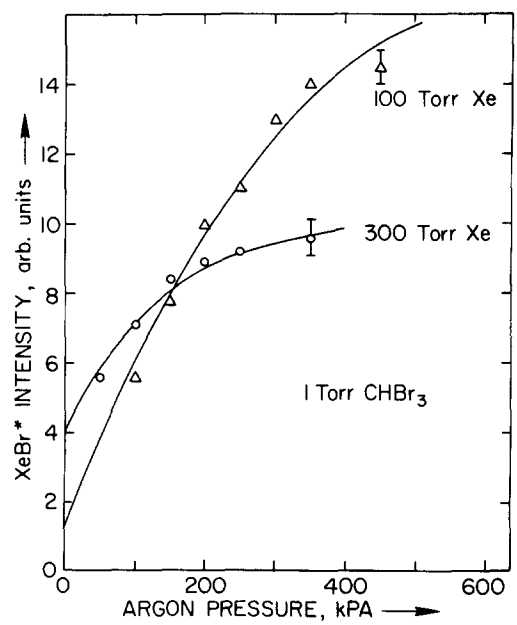

FIG. 6. XeBr* fluorescence peak intensity as a function of argon pressure for two different xenon pressures; (a) 100 Torr and (b) 300 Torr with 1 Torr $CHBr_3$. The solid lines are a fit of Eq. (12) to the data.

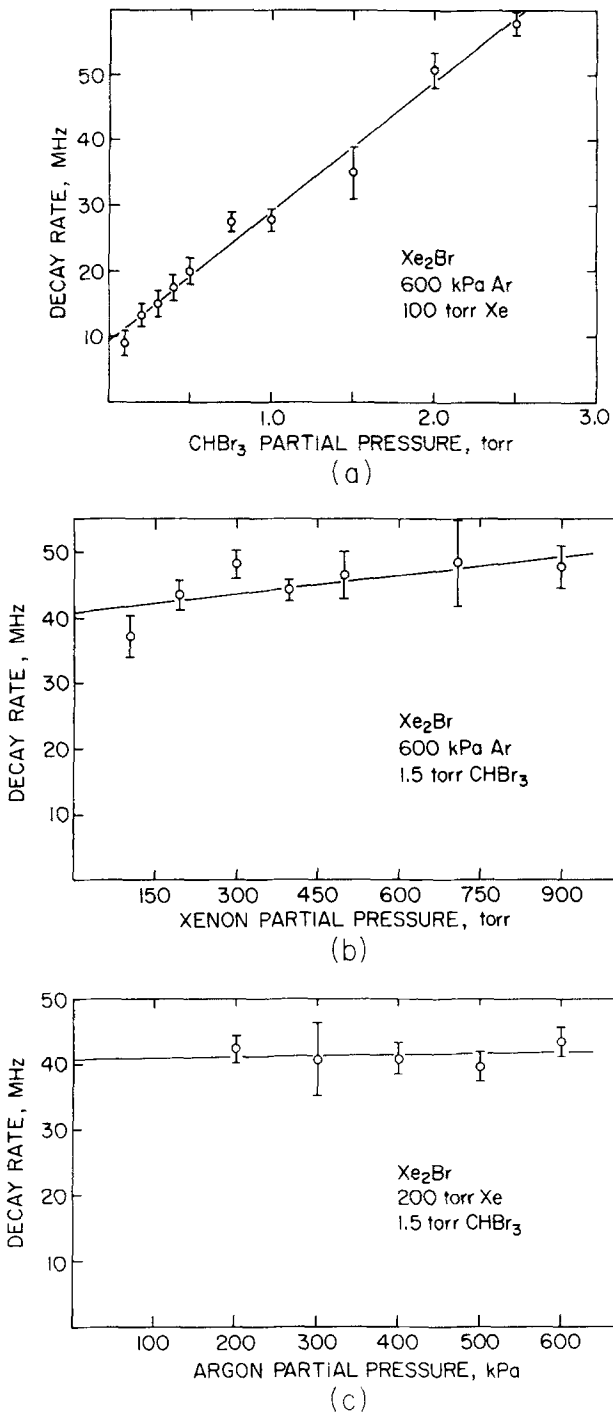

FIG. 7. Variation of decay rates ($1/\tau_{eff}$) for Xe_2Br^* emission at 440 nm as a function of (a) $CHBr_3$ pressure, (b) xenon pressure and (c) argon pressure.

TABLE II. Xe_2Br^* quenching rates of bromine donors.

Donor	Quenching rate k_q ($cm^3\,s^{-1}$)
CBr_4	3.2×10^{-10}
$CHBr_3$	5.6×10^{-10}
HBr	6.5×10^{-11}
Br_2	3.3×10^{-10}
CH_3Br	8.0×10^{-10}
C_2H_5Br	7.4×10^{-10}

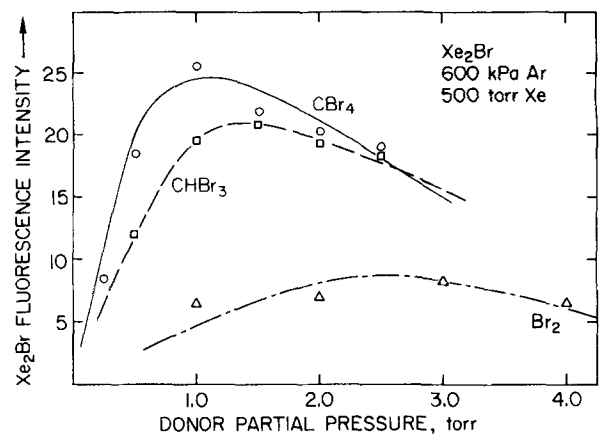

FIG. 8. Comparison of Xe_2Br^* fluorescence as a function of donor pressure for $CHBr_3$, CBr_4, and Br_2 donors, with 500 Torr of xenon and 600 kPa of argon.

bromide. Although HBr had reasonable yield, it was very reactive and hydroscopic making it difficult to obtain useful experimental information about its properties. Figure 8 depicts the fluorescence yield of three different donors as a function of donor pressure.

DISCUSSION

The production process for Xe_2Br^* is essentially a three-body quenching process of $XeBr^*$. Unlike the case of Xe_2Cl^*, where the three-body quenching of $XeCl^*$ is much larger than the production rate of Xe_2Cl^*,[24] these values are equal to within experimental error for Xe_2Br^*. This means that there is a very high production efficiency for Xe_2Br^* from $XeBr^*$, of more than 75%.

In order to explain the difference between the three body quenching rate of $XeCl^*$ and formation rate of Xe_2Cl^*, an intermediate species, $ArXeCl^*$ was suggested.[24] No evidence was found which would suggest that an analogous molecule ($ArXeBr^*$) was being formed in our experiments.

Because of the large energy difference between Xe_2Br^* and $2Xe+Br(^2P_{3/2})$ or $2Xe+Br(^2P_{1/2})$, the cross section for a quenching process yielding the atomic products should be quite small.[28] Therefore, Xe_2Br^* formation is the only important channel for a three-body quenching reaction of $XeBr^*$. As a result, the three-body quenching of $XeBr^*$ by 2Ar should be negligible. Indeed, no evidence for removal of $XeBr^*$ by 2Ar was found in our experiments.

For the reaction of $XeBr^*$ with two Xe atoms, only the quenching constant for $XeBr^*$ was measured. However, the arguments cited above for the Ar–Xe reaction hold for the Xe–Xe reaction as well. Therefore, it may be supposed that the production rate for Xe_2Br^* by this process has about the same magnitude as the quenching rate of $XeBr^*$ by 2Xe.

No evidence for the production of Xe_2Br^* via Xe_2^* was observed. Even if this process does occur, its contribution to the total Xe_2Br^* population seems to be negligible under the present experimental conditions.

The analysis of the three-body quenching of XeBr* was founded on the assumption that the production efficiency of XeBr* was independent of both the argon and xenon pressure. If this assumption is correct, than the ratio of the production constants f_2/f_1 should depend only on the ratio of the excited and ionized argon and xenon species initially created by the e-beam excitation. Taking into account the different stopping powers for Xe and Ar and the energy necessary to create either Ar^+ or Xe^+, respectively, the ratio f_2/f_1 should equal about three. The ratio f_2/f_1 which gives the best fit to Figs. 5 and 6 is 2.45. This is a reasonable agreement, and supports the assumption that the production rate P depends only on the ratio of the density of excited species.

Quenching of XeBr* by electrons has been neglected in our analysis because no information about this process is available. However, calculations by Hazi *et al.*[29] and experimental investigations by Trainor and Jacob[30] for the rare gas fluorides suggest a rate constant on the order of 10^{-7} $cm^3 s^{-1}$ for the quenching of these molecules by superelastic collisions. Using this rate constant with XeBr* indicates that in the low pressure regions in Figs. 5 and 6, the results might be somewhat influenced by electron quenching. However, for the higher pressures, the three body quenching strongly dominates. The excellent fit to the experimental results shown in Figs. 6 and 7 by Eqs. (11) and (12) supports the assumption that all of the important reactions have been included in the model. The uncertainty in the values of (k_3+k_4) and (k_5+k_6) is partly due to the uncertainty in f_2/f_1, as well as from a possible error in the determination of τ_{282} and k_2.

The quenching constants (Table II) for $CHBr_3$, CH_3Br, and Br_2 are accurate to within about 20%. Because of the experimental difficulties associated with HBr, the reproducibility of the data for this donor was not quite as good. An error of about 30% can be estimated in this case. CBr_4 had to be heated to yield a reasonable vapor pressure. Thus, the donor pressure measurement was somewhat uncertain, causing an uncertainty in the quenching rate for CBr_4 of about a factor of 2. The fluorescence intensities observed with the different donors (Fig. 8) are not correlated with the quenching rates for each donor, indicating much different production efficiencies for XeBr* by the various donors. Only the quenching rates for the three donors yielding the most reliable results were used in the determination of the radiative lifetime of Xe_2Br^*.

From the results of these measurements, it is possible to make an estimate of the stimulated emission cross section and gain which one might expect for e-beam excited Xe_2Br^*. Using the radiative lifetime τ_{Xe_2Br} of 245 ns, and a fluorescence emission bandwidth (FWHM) of 65 nm a cross section of about 2.5×10^{-18} cm^2 was calculated. Thus, if competing absorption effects are neglected and an excited species density of 4×10^{15} cm^{-3} could be achieved,[5] a gain of 1% cm^{-1} would be expected.

In summary, the kinetic processes leading to the formation and removal of Xe_2Br^* in electron beam excited mixtures of Ar/Xe/RBr have been studied. A termolecular reaction involving XeBr*, Xe, and Ar has been identified as the primary formation mechanism, and the pertinent reaction rates and radiative lifetimes measured.

ACKNOWLEDGMENTS

The authors would like to thank G. Zhehuna for experimental assistance, as well as many helpful discussions with Dr. G. P. Glass. This research is jointly supported by the Office of Naval Research, the National Science Foundation, and the Robert A. Welch Foundation. One of us (R.S.) would like to acknowledge support by the Deutsche Forschungsgemeinschaft.

[1]D. C. Lorents, D. L. Huestis, G. V. McCusker, H. H. Nakano, and R. M. Hill, J. Chem. Phys. **68**, 4657 (1978).
[2]J. A. Mangano, J. H. Jacob, M. Rokni, and A. Hawryluk, Appl. Phys. Lett. **31**, 26 (1977).
[3]N. G. Basov, V. A. Danilychev, V. A. Dolgika, O. M. Karimov, V. S. Lebedev, and A. G. Molchanov, JETP Lett. **26**, 16 (1977).
[4]J. G. Eden, R. S. F. Chang, and J. L. Palumbo, IEEE J. Quantum Electron. **QE-15**, 1146 (1979).
[5]F. K. Tittel, G. Marowsky, W. L. Wilson, Jr. and M. C. Smayling, IEEE J. Quantum Electron. **QE-17**, 1488 (1981).
[6]J. A. Mangano, J. H. Jacobs, M. Rokni, and A. Hawryluk, Appl. Phys. Lett. **31**, 26 (1977).
[7]M. Rokni, J. H. Jacobs, J. A. Mangano, and R. Bochu. Appl. Phys. Lett. **30**, 458 (1977).
[8]D. C. Lorents, R. M. Hill, D. L. Huestis, M. V. McCusker, and H. H. Nakano, in *Electronic Transition in Lasers*, edited by L. F. Wilson, S. N. Suchard, and J. I. Steinfeld (Massachusetts Institute of Technology, Cambridge, 1977).
[9]D. L. Huestis and N. E. Schlotter, J. Chem. Phys. **69**, 3100 (1978).
[10]D. L. Huestis, Topical Meeting on Excimer Lasers, Sept. 11–13, 1979, Charleston, South Carolina.
[11]K. Y. Tang, D. C. Lorents, and D. L. Huestis, Appl. Phys. Lett. **36**, 347 (1980).
[12]F. K. Tittel, W. L. Wilson, R. E. Stickel, G. Marowsky, and W. E. Ernst, Appl. Phys. Lett. **36**, 405 (1980).
[13]F. K. Tittel, M. Smayling, W. L. Wilson, and G. Marowsky, Appl. Phys. Lett. **37**, 862 (1980).
[14]J. E. Valazco and D. W. Setser, J. Chem. Phys. **62**, 1990 (1975).
[15]C. A. Brau and J. J. Ewing, J. Chem. Phys. **63**, 4640 (1975).
[16]S. K. Searles and G. A. Hart, Appl. Phys. Lett. **27**, 243 (1975).
[17]I. N. Konovalov, V. F. Losev, V. V. Ryzhov, V. F. Tarasenko, and A. G. Tostremskii, Opt. Spectrosc. (USSR) **47**, 137 (1979), also *Proceedings of the International Conference on Lasers*, 1980 (STS, New Orleans, 1980), p. 686; J. Tech. Phys. (USSR) 50, 350 (1980).
[18]G. Marowsky, R. Cordray, F. K. Tittel, and W. L. Wilson, Appl. Opt. **17**, 3491 (1978).
[19]C. H. Chen and M. G. Payne, Appl. Phys. Lett. **32**, 358 (1978).
[20]G. P. Quigley and W. M. Hughes, Appl. Phys. Lett. **32**, 649 (1978).
[21]G. Marowsky, G. P. Glass, F. K. Tittel, K. Hohla, W. L. Wilson, and H. Weber, IEEE J. Quantum Electron. QE-18, 889 (1982).
[22]N. Bowering, R. Sauerbrey, and H. Langhoff, J. Chem. Phys. **76**, 3524 (1982).
[23]G. P. Glass, M. Smayling, F. K. Tittel, and W. L. Wilson, Jr., J. Chem. Phys. **75**, 1153 (1981).
[24]G. P. Glass, F. K. Tittel, W. L. Wilson, Jr. and M. C.

Smayling, Chem. Phys. Lett. 83, 585 (1981).
[25]K. Y. Tang, D. C. Lorents, and D. L. Huestis, *Proceedings of the International Conference on Lasers*, 1980 (STS, New Orleans, 1981), p. 692.
[26]J. Maya and P. Davidovits, J. Chem. Phys. 59, 3143 (1973).
[27]C. A. Hart and S. K. Searles, J. Appl. Phys. 47, 2033 (1976).
[28]E. E. Nikitin, Chem. Phys. Lett. 2, 402 (1968).
[29]A. U. Hazi, T. N. Rescigno, and A. E. Orel, Appl. Phys. Lett. 35, 477 (1979).
[30]D. W. Trainor and J. H. Jacob, Appl. Phys. Lett. 37, 675 (1980).